

## **FRICITION COEFFICIENT DISPLAYED BY SLIDING SURFACES LUBRICATED BY SAND CONTAMINATED OIL**

**Al-Osaimy A. S.**

**Faculty of Engineering, Taif University, Al – Taif, SAUDI ARABIA.**

The present work discusses the effect of sand particles, contaminated in the lubricating oil, as well as sand particles embedded in the sliding surfaces, on the friction coefficient displayed by polyamides sliding against steel. Stribeck curve is used to compare the friction performance in boundary, mixed and hydrodynamic regimes. Experiments were carried out to investigate the friction coefficient of the tested materials when the oil was contaminated by sand particles of different particle sizes and contents.

In the presence of sand particles, the friction increase was attributed to the abrasion of the sliding surfaces by sand particles. In the mixed lubrication regime, the combined effects between boundary and hydrodynamic lubrication was controlling friction coefficient for clean oil. The minimum friction coefficient appears in the mixed lubrication regime. Sand particles in oil disturbed the hydrodynamic film and altered the values of friction coefficient. It was observed that friction coefficient with sand particles was higher than that displayed by clean oil. The presence of sand particles in the oil and as embedded particles in the sliding surfaces strongly affected the friction coefficient. Only when the sand particle size was higher than the film thickness and the particles were embedded into one surface and cut into the other one abrasion occurred and friction coefficient increased.

### **KEYWORDS**

**Stribeck curve, friction coefficient, sand particle, oil, polyamide, steel.**

### **INTRODUCTION**

In desert areas, abrasive particles entering the machines cause serious wear of the sliding components. It is essential to reduce friction and improve the wear resistance of the machine parts. Most of the work conducted on lubricated surfaces assume lubricants free of sand particles. Few works were forwarded into the effect of sand particles on friction and wear of lubricated surfaces. Three body abrasive wear can be classified into two types: with rolling particle motion and with grooving particle motion. Wear modes in the micro-scale abrasion test can be changed from ‘three-body’ abrasion (with rolling particle motion) to ‘two-body’ abrasion (with grooving particle motion) by changing the load, [1], the volume fraction of abrasive in the slurry, [2], the abrasive particles, the materials of ball and specimen, and the ball surface condition, [3]. A critical condition was proposed for the transition from ‘three-body’ to ‘two-body’ abrasion. Three-body abrasion is, however, much more complicated than two-body abrasion. It has been concluded, [4 - 8], that the movement patterns for abrasive particles can be exactly

defined as sliding and rolling. When abrasive particles slide, the wear pattern is the same to two-body abrasion. When abrasive particles roll, the wear will predominantly depend upon plastic deformation behavior, that is, low-cycle fatigue mechanism of material. Because there are lot of particles to roll in three-body abrasion, plastic deformation wear will be much more important in three-body abrasion than that in two-body abrasion.

The wear and friction of cylindrical contacts caused by lubricant abrasive was reported, [9]. Different particle size abrasive as well as the abrasive used for testing of automotive oil filters and air cleaners were added to the lubricant. The experiments show that three body abrasive wear is mainly dependent on the embed ability of abrasive in the rubbing surfaces. The embedment of the abrasive particles is classified into weak, partial and complete. The effect of both antiwear and dispersant lubricant additives on wear and friction caused by lubricant abrasive contaminants was tested, [10]. Dispersant additive has been added to the base oil with/without antiwear additives such as ZDTP and CMOC. It can be concluded that, for base oil containing only dispersant additive, wear and friction slightly increased with increasing the concentration of dispersant additive. While for base oil containing both of dispersant and antiwear additives, wear decreased significantly with increasing dispersant additive concentration. Experiments have been carried out to test the friction and wear of piston ring specimen and cylinder liner, constructed in a test model. Abrasive contaminants of different particle sizes were added to the oil at controlled concentrations. On the basis of the obtained results, [11], the effect of abrasive particle size on wear and friction was described and the required filter fineness was recommended.

The historical development on the discoveries of lubrication regimes for lubricated sliding contacts has been reviewed from the very beginning, [12]. It was found that the functional relationship between the coefficient of friction and the product of sliding speed and viscosity divided by the normal load well known as the Stribeck curve has been experimentally explored much earlier by Adolf Martens in 1888 long before Richard Stribeck did his pioneering measurements in 1902.

The viscosity of a fluid is used to describe the resistance of relative movement between flow-layers and determine its performance in friction reduction, [13]. When solid additives are added into a lubricant, fluid drag that acts on a solid surface affects the fluid viscosity and the hydrodynamic pressure. It has been reported that the shape of an additive affects the amount of fluid drag, [14, 15]. The additives that align in the fluid direction could reduce the fluid drag, [16, 17]. When nanoplatelets are utilized as lubricant (mineral oil and water) additives, the enhancement in the lubrication is found via modification of lubricants rheological performance.

The tribological behavior of oil lubricated DLC coated surfaces under the conditions without and with sand particles was investigated, [18]. The effects of applied load, frequency, and sand particles on the tribological performance of DLC coating were systemically studied. The analysis results showed that solid-liquid lubricating coatings including the tested lubricant exhibited excellent antifriction but relative poor wear resistance performances under the conditions without and with sand environments. The added sand particles lead to the wear rates to the one order of magnitude large than that without sand conditions for all the selected liquid lubricants. The viscosity, contact angle

and work of adhesion played an important part in affecting the tribological performances. The lubrication regimes in Stribeck curve for the five kinds of liquid lubricants were affected obviously by the sand particles in different way. The formed transfer films on the coating surface and pin have much influence on the tribological behavior and the transition between lubrication regimes.

The wear debris and foreign particles like sand-dust are the very important influencing factor to affect the lifetime of the oil lubricating mechanical system. In addition, there are a large number of sand-dust regions all over the world accounting for about 21% of total land area of the world. Sand-dust, by way of producing severe abrasive wear, can cause catastrophic failure between the two interacting surfaces in the relative motion, [19, 20]. However, the reports on the tribological properties of DLC under oil conditions are hard to find, especially in the complex system combined oil, solid lubricant coating and sand. The tribological performance of graphite-like carbon (GLC) coatings combined with five types of liquid lubricants has been investigated under the conditions without and with sand particles, [21]. Experimental results showed that the obtained excellent low friction and wear resistance was attributed to the synergistic effect of liquid lubricant sand GLC coatings.

In the present work, the effect of sand particles, contaminated in the lubricating oil, as well as sand particles embedded in the sliding surfaces on the friction coefficient for polyamides sliding against steel is investigated.

## EXPERIMENTAL

Experiments were carried out using wear tester, Fig. 1. Test specimens were of polyamide (PA 6) in form of cubes of  $20 \times 20 \times 20$  mm. The sliding surface of the test specimens was ground by an emery paper of 500 grades before test. The counterface, in form of stainless steel disc of 40 mm diameter and 11 mm width, was fastened to the rotating shaft of the tester. Load was applied by weights. The sliding velocity was varied in the range of 0.4 – 1.2 m/s and the load was varied between 1.0 and 240 N. The experiments were performed under laboratory conditions (25° C temperature and 30% humidity) using a block on ring rig assembled in Amsler testing machine. The effects of sliding velocity and load on the friction coefficient of the tested material pairs were studied. Friction coefficient was determined by measuring the friction torque using a pendulum device, which is a part of Amsler machine.

The tested oil (S. A. E. 30) was prefiltered by 0.45  $\mu\text{m}$  filter. Oil was supplied to the contact area by gravity. Sand particles of single cut of 0 – 10  $\mu\text{m}$ , 0 - 25  $\mu\text{m}$ , 0 - 50  $\mu\text{m}$ , 0 - 100  $\mu\text{m}$  and 0 - 200  $\mu\text{m}$  sizes were tested. They were added to the oil in 0.5 g/l and 1.0 g/l concentration. The rings, of 40 mm diameter and 10 mm width, made from stainless steel {403 S17 (12 % Cr, 0.5 Ni %, 1.0%, Mn, 0.8% Si)} slide against a block, in form of polyamide cube, ( $20 \times 20 \times 20$  mm). The surface roughness of the test specimens that were finished by grinding was 3.4  $\mu\text{m}$   $R_a$ , while the roughness of the stainless steel ring was 0.17  $\mu\text{m}$   $R_a$ . The tested block was held in the stationary shaft, while stainless steel discs were assembled to the rotating shaft. Based on the analysis of the friction coefficient under different loads and sliding velocities, the Stribeck curves were presented for all tested conditions.

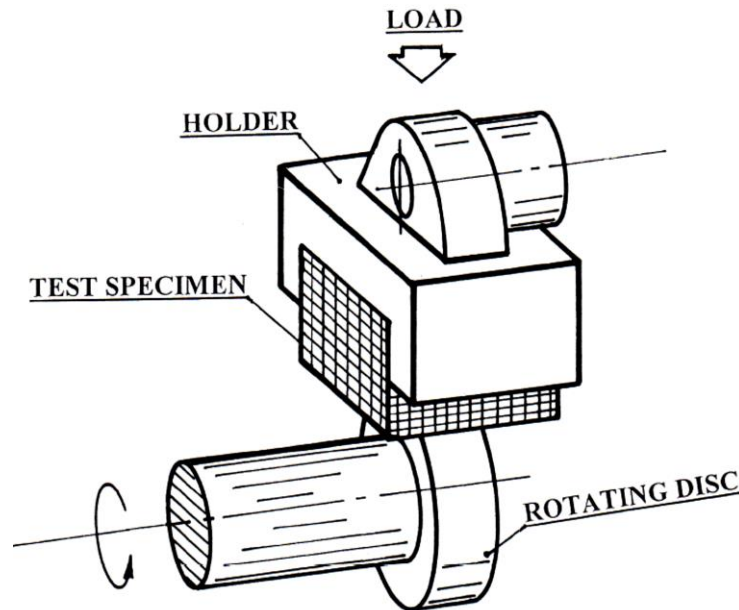


Fig. 1 Arrangement of the test rig.

## RESULTS AND DISCUSSION

The experiments discuss the frictional performance of the lubricated surfaces by Stribeck curve which expresses the relationship between the friction coefficient, viscosity of the lubricating fluid  $[\eta]$ , load per unit length  $[F]$ , and velocity  $[U]$ . The curve illustrates the characteristics of various lubrication regions, including boundary lubrication (BL), mixed lubrication (ML) and elastohydrodynamic lubrication (EHL). These three parameters are included in Stribeck curve which contains three lubrication regimes. The first regime is the boundary lubrication regime (BL) where the film thickness equals zero. While in the mixed lubrication regime (ML), where the oil film is lower than the surface roughness, the slope is negative. The third regime is the hydrodynamic lubrication (EHL), where the oil film is higher than the surface roughness, the slope is positive. The minimum value of friction coefficient is observed in the mixed lubrication regime (ML). As the sliding velocity increases the oil film increases and consequently friction coefficient increases.

The effect of sand particles, of 0.5 g/l concentration contaminated in the oil, on friction coefficient is shown in Fig. 3. Slight friction increase was observed for sand particles of 0 – 10  $\mu\text{m}$ . As the particle size increased friction coefficient increased. The highest friction values were detected in the presence of sand of 0 – 200  $\mu\text{m}$  particle size. It seems that as the particle size exceeds the oil film thickness, the interaction of the sand and the PA 6 as well the steel surfaces increased causing friction increase which was more obvious in ML regime than EHL one, where oil film thickness was smaller than sand particle size.

As the sand particles concentration increased up to 1.0 g/l, friction coefficient significantly increased, Fig. 4. The highest friction value (1.9) was recorded at ML in the presence of 0 – 200  $\mu\text{m}$  particle size, while the lowest value (0.73) was observed in the EHL area. The regimes of ML and EHL are identified in the curve. In the EHL regime, it seems that the solid–solid contacts were accelerated by sand particles. On the mixed lubrication regime with dominating asperity solid–solid contacts, the interaction of sand

particles was significantly noted, where sand particles were able to break the lubricating film.

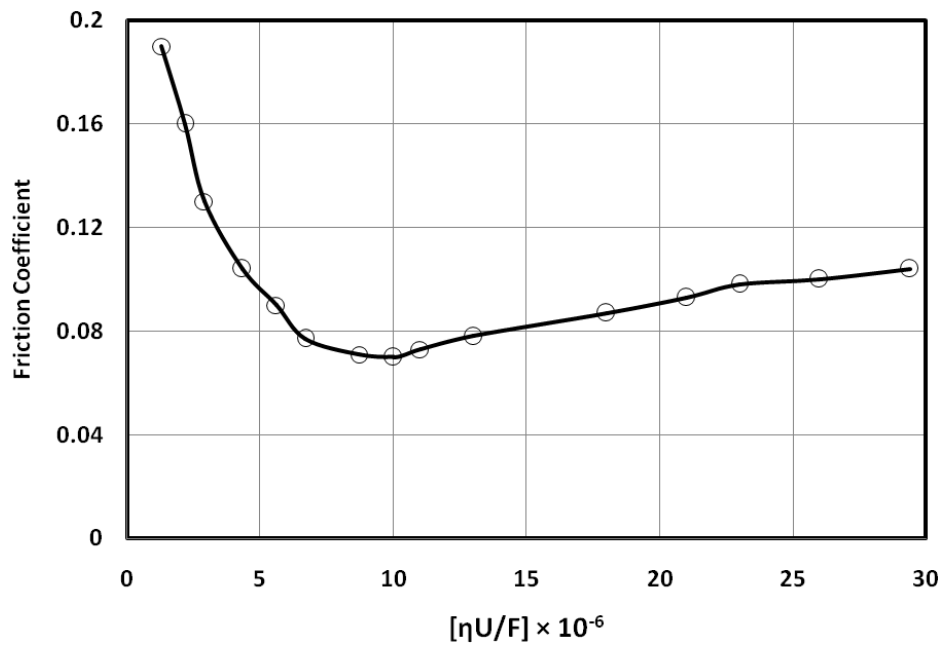


Fig. 2 The relationship between friction coefficient and Sommerfeld number for clean oil.

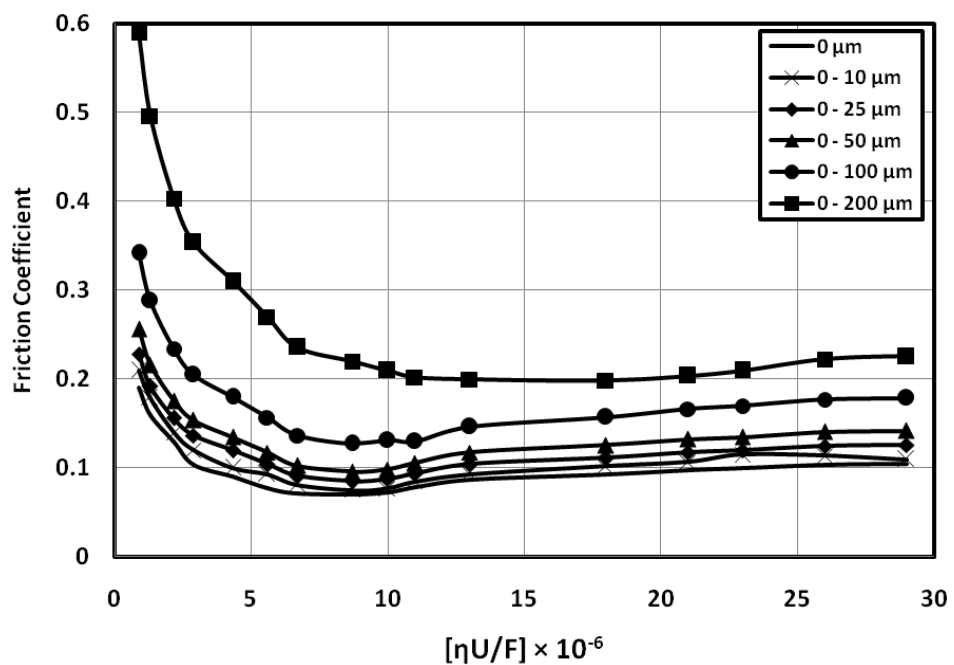
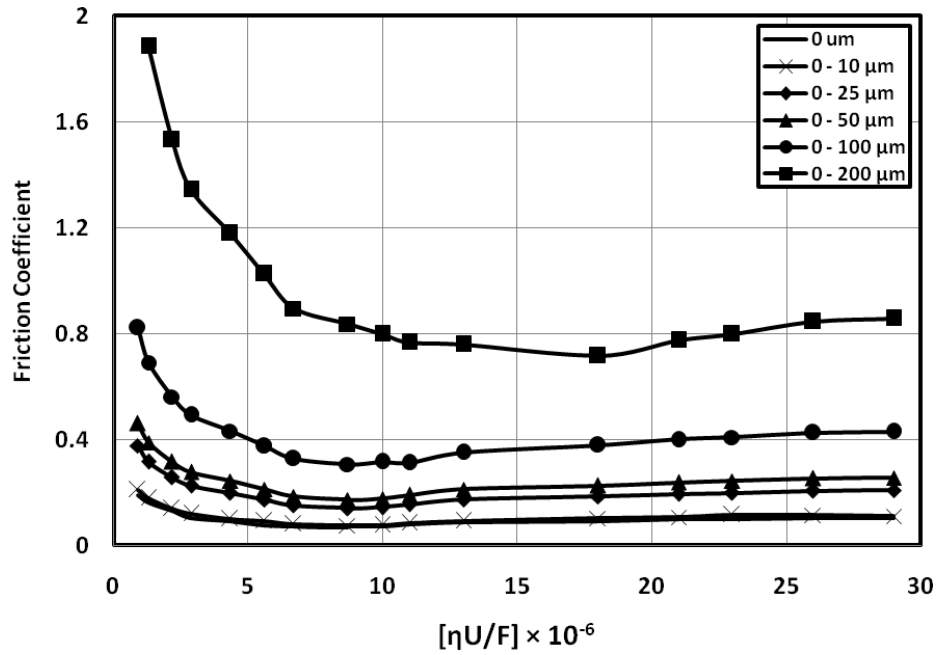


Fig. 3 The relationship between friction coefficient and Sommerfeld number for contaminated oil of 0.5 g/l sand particles concentration.



**Fig. 4** The relationship between friction coefficient and Sommerfeld number for contaminated oil of 1.0 g/l sand particles concentration.

Experiment were carried out to determine the friction coefficient using clean oil after running with contaminated oil. The results of the experiments that illustrated the effect of the sand embedded particles during running using sand contaminated oil on friction coefficient are shown in Figs. 5 – 10. The effect of sand particle size of 0 – 200  $\mu\text{m}$  and 0.5 g/l concentration that embedded in the surface of PA 6 on friction coefficient is shown in Fig. 5. Compared to clean oil, the friction coefficient showed an increase in both ML and EHL regimes. This behavior was due to abrading action of the embedded sand particles into the surfaces of PA 6 and steel.

Friction coefficient displayed by clean oil after embedment by sand of 0 – 200  $\mu\text{m}$  particle size and 0.5 g/l concentration is shown in Fig. 6, where the values were lower than that observed for 0 – 200  $\mu\text{m}$  particle size. As the particle size decreased, the effect of the embedded particles decreased.

When the concentration of sand particles increased up to 1.0 g/l, friction coefficient showed relative increase, Fig. 7. This behavior confirmed the fact that embedment was influenced by the concentration and particle size of sand particles.

Friction coefficient displayed by clean oil after embedment by sand of 0 – 200  $\mu\text{m}$  particle size and 1.0 g/l concentration, Fig. 8, showed relatively lower values than that observed in the presence of 0 – 200  $\mu\text{m}$  sand particle size. Further friction decrease was observed as the particle size decreased to 0 – 50  $\mu\text{m}$ , Fig. 9. The lowest friction value was 0.09, while the highest one was 0.4 displayed in ML regime.

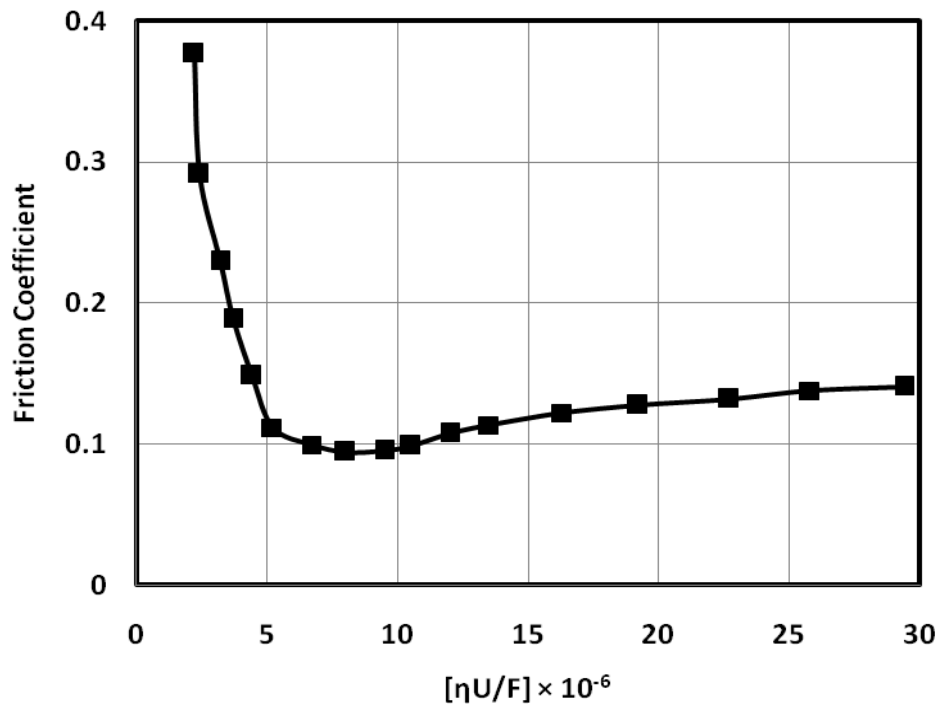


**Fig. 5 Friction coefficient displayed by clean oil after embedment by sand of 0 – 200 μm particle size and 0.5 g/l concentration.**

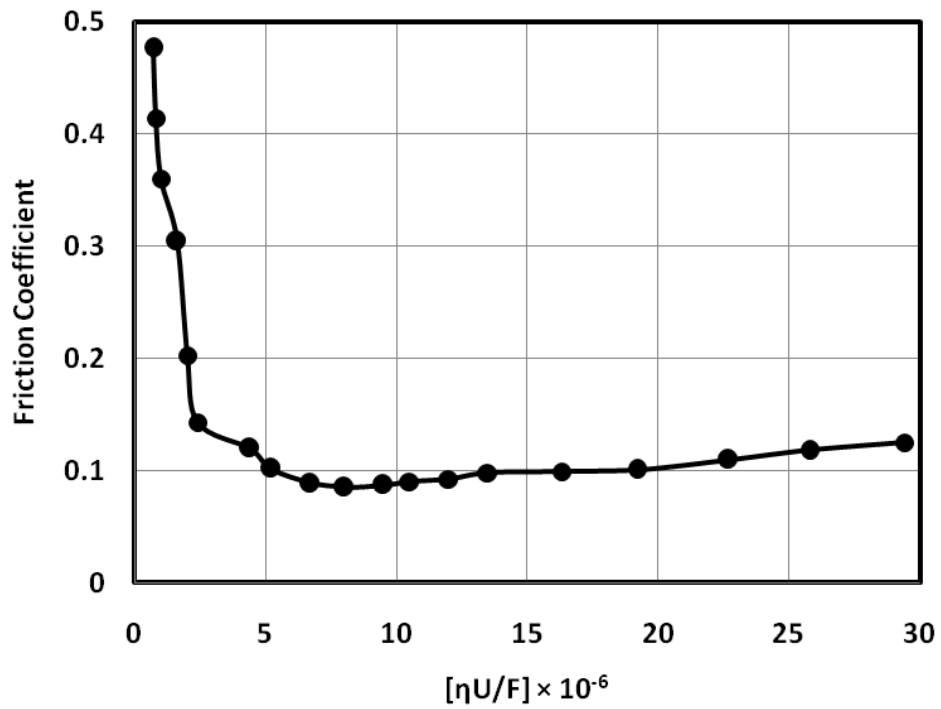


**Fig. 6 Friction coefficient displayed by clean oil after embedment by sand of 0 – 100 μm particle size and 0.5 g/l concentration.**

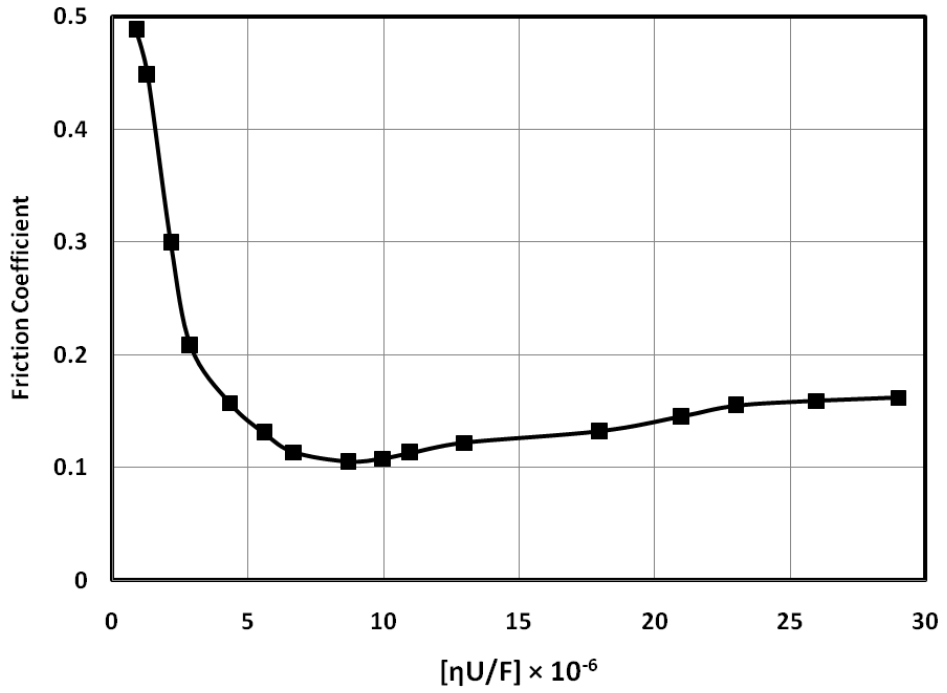


**Fig. 7 Friction coefficient displayed by clean oil after embedment by sand of 0 – 200 μm particle size and 1.0 g/l concentration.**

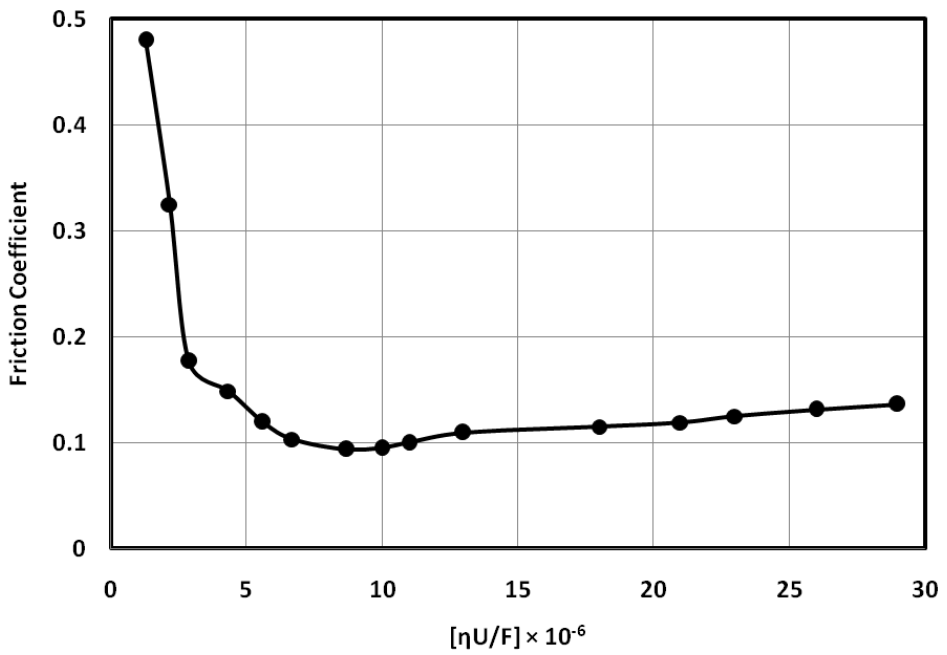


**Fig. 8 Friction coefficient displayed by clean oil after embedment by sand of 0 – 100 μm particle size and 1.0 g/l concentration.**

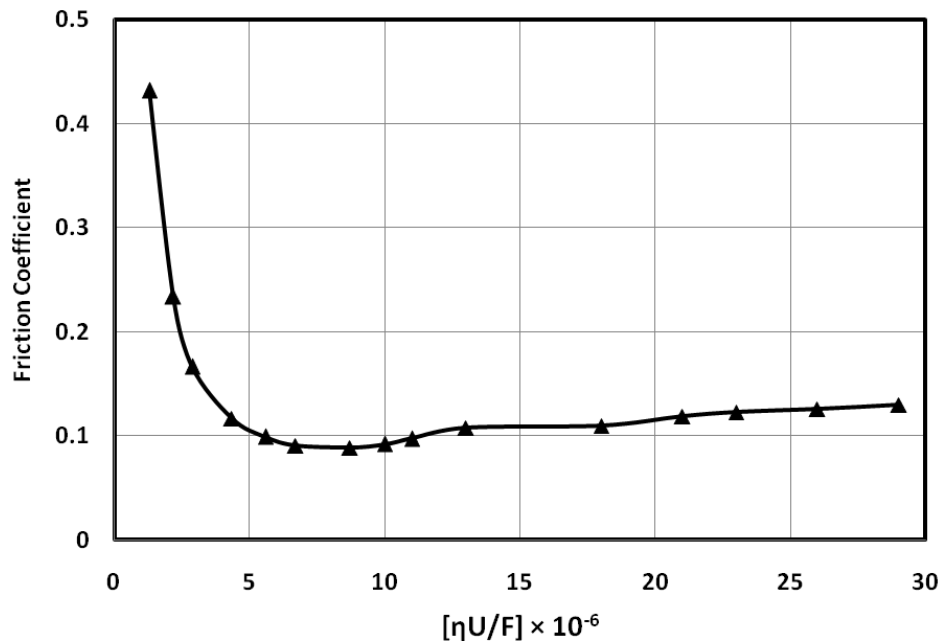


**Fig. 9 Friction coefficient displayed by clean oil after embedment by sand of 0 – 50 μm particle size and 1.0 g/l concentration.**

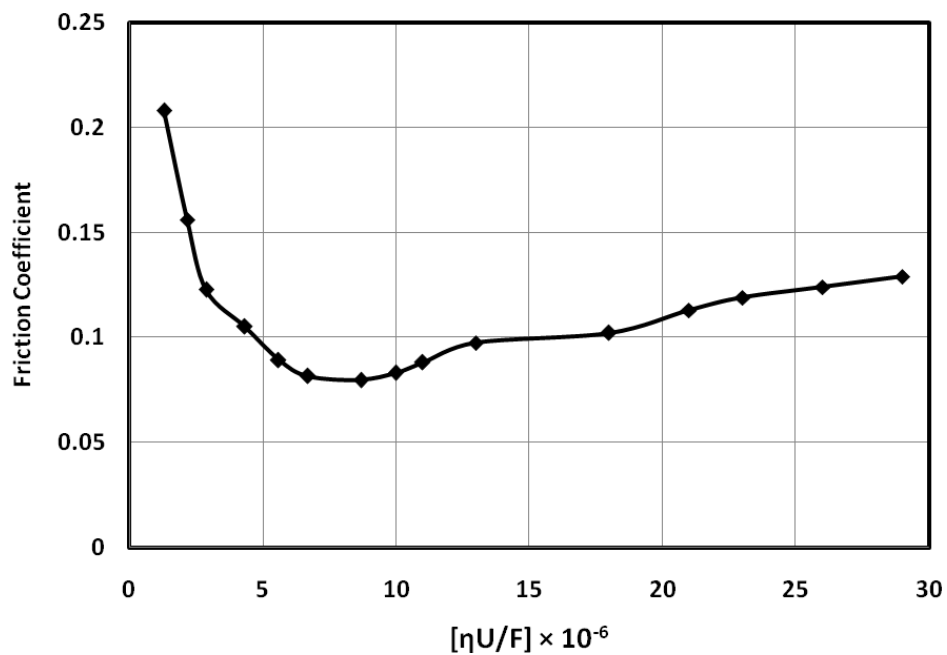
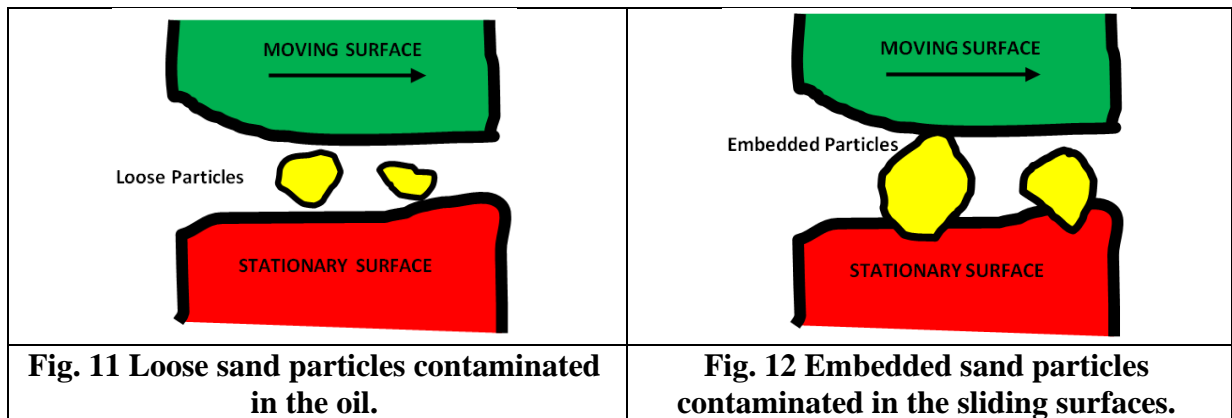


**Fig. 10 Friction coefficient displayed by clean oil after embedment by sand of 0 – 25 μm particle size and 1.0 g/l concentration.**

Friction coefficient displayed by clean oil after embedment of 0 – 50 μm sand particles and 1.0 g/l concentration showed further friction decrease, Fig. 9. The lowest friction value was 0.085 at  $8 \times 10^{-6}$  Sommerfeld number in ML regime. For sliding surfaces ran only with clean oil, the lowest friction coefficient was 0.072 at the same value of Sommerfeld number. The highest friction value was 0.43 in ML regime. As for surfaces ran with oil contaminated by sand particles of 0 – 25 μm size and 1.0 g/l concentration,

Fig. 10, friction coefficient showed the lowest values. Sand particle size of 0 – 10  $\mu\text{m}$  had no effect on friction coefficient.



For clean oil, in hydrodynamic lubrication, the asperities of the surface roughness do not touch but are separated by a lubricant film in which very low shear occurs resulted from the oil layers. In the presence of sand particles, the friction increase was attributed to the abrasion of the sliding surfaces by sand particles. In the mixed lubrication regime, the combined effects between boundary and hydrodynamic lubrication was controlling friction coefficient for clean oil. The minimum friction coefficient appears in the mixed lubrication regime. Sand particles in oil disturbed the hydrodynamic film and altered the value of friction coefficient. It was observed that friction coefficient with sand particles was higher than that observed for clean oil.

The presence of sand particles circulating in the oil and as embedded particles in the sliding surfaces strongly affected the friction coefficient. For loose particles which their particle size was smaller than oil film thickness, Fig. 11, friction coefficient was not affected by those particles. Only when the sand particles size was bigger than oil film thickness, Fig. 12, they stuck to one surface and cut into the other then abrasion occurred. During the cutting process caused by sand particles, friction coefficient significantly increased. The friction value fluctuated violently at the commencement of sand particle microcutting in both of the sliding surfaces.

## CONCLUSIONS

Slight friction increase was observed for sand particles of 0 – 10  $\mu\text{m}$ . As the particle size increased, friction coefficient increased. The highest friction values were detected in the presence of sand of 0 – 200  $\mu\text{m}$  particle size. It seems that as the particle size exceeds the oil film thickness, the interaction of the sand and the PA 6 as well the steel surfaces increased causing friction increase, which was more obvious in ML regime than EHL one. As the sand particles concentration increased up to 1.0 g/l, friction coefficient significantly increased. The highest friction value (1.9) was recorded at ML in the presence of 0 – 200  $\mu\text{m}$  particle size, while the lowest value (0.73) was observed in the EHL area. On the mixed lubrication regime with dominating asperity solid–solid contacts, the interaction of sand particles was significantly noted, where sand particles were able to break the lubricating film.

Friction coefficient using clean oil after running with contaminated oil showed an increase in both ML and EHL regimes. The effect of the sand particles, of 0 – 200  $\mu\text{m}$  sand particles and 0.5 g/l concentration that embedded in the surface of PA 6, on friction coefficient was higher than that displayed by 0 – 100  $\mu\text{m}$  sand particles and 0.5 g/l concentration. As the sand particle size decreased, the effect of the embedded particles decreased. When the concentration of sand increased to 1.0 g/l, friction coefficient showed relative increase. This behavior confirmed the fact that embedment was influenced by the concentration and particle size of sand particles. Friction coefficient, displayed by clean oil after embedment by sand particles of 0 – 100  $\mu\text{m}$  size and 1.0 g/l concentration, showed relatively lower values than that observed in the presence of 0 – 200  $\mu\text{m}$  particle size. Further friction decrease was observed as the particle size decreased to 0 – 50  $\mu\text{m}$ . The lowest friction value was 0.09, while the highest one was 0.4 in ML regime. The lowest friction value was 0.085 at  $8 \times 10^{-6}$  Sommerfeld number in ML regime. For sliding surfaces ran only with clean oil the lowest friction coefficient was 0.072 at the same value of Sommerfeld number.

## REFERENCES

1. Trezona R. I., Hutchings I. M., "Three-body abrasive wear testing of soft materials", *Wear* 233 - 235, pp. 209 - 221, (1999).
2. Allsopp D. N., Trezona R. I., Hutchings I. M., "The effects of ball surface condition in the micro-scale abrasive wear test", *Tribol. Lett.*5, pp. 259 - 264, (1998).
3. Adachi K., Hutchings I., "Wear-mode mapping for the micro-scale abrasion test", *Wear* 255, pp. 23 - 29, (2003).
4. Fang L., Liu W., Du D., Zhang X., Xue Q., "Predicting three-body abrasive wear using Monte Carlo methods", *Wear* 256, pp. 685 - 694, (2004).
5. Fang L., Kong X. L., Su J. Y., Zhou Q. D., "Movement patterns of abrasive particles in three-body abrasion", *Wear* 162 - 164, pp. 782– 789, (1993).
6. Fang L., Zhou Q. D., "A statistical model describing wear traces in three-body abrasion", *Tribotest* 2, pp. 47 - 53, (1995).
7. Fang L., Zhou Q. D., Rao Q. C., "An experimental simulation of cutting wear in three-body abrasion", *Wear* 218, pp. 188 - 194, (1998).
8. Nicholls J. R., Stephenson J. R., "Monte Carlo modeling of erosion processes", *Wear* 186, pp. 64 - 77,(1995).
9. Ali W. and Mousa, M., "Wear and Friction of Cylindrical Contacts by Lubricant Abrasive Contaminants", *Proceedings of EGTRIB First Tribology Conference, Dec. 20 - 21, 1989, Cairo, Egypt, (1989).*
10. Mousa M. O., Balogh I. and Ali W. Y., "Effect of Lubricant Additives on Wear and Friction Caused by Lubricant Abrasive Contaminants", *Proceedings of XXI Bus Meeting, Budapest, September 3 - 6, 1990, pp. 197 - 204, (1990).*
11. Mousa M. and Ali W., "Particle Size Effect on Friction and Wear Caused by Abrasive Contaminants in Lubricating Oil", *3rd Int. Ain-Sham Univ. Conf., Cairo. Dec. 27 - 29, pp. 213 - 222, (1990).*
12. Woydt M., Wäsche R., "The history of the Stribeck curve and ball bearing steels: The role of Adolf Martens", *Wear* 268, pp. 1542 – 1546, (2010).
13. He X., Xiao H., Choi H., Díaz A., Mosby B., Clearfield A., Liang H., " $\alpha$ -Zirconium phosphate nanoplatelets as lubricant additives", *Colloids and Surfaces A: Physicochem. Eng. Aspects* 452, pp. 32 – 38, (2014).
14. Herrmann H., Araújo A.D., Almeida M.P., "Particles in fluids", *Eur. Phys.J. Special Top.* 143, pp. 181 – 189, (2007).

15. Leal L. G., "Particle motions in a viscous fluid", *Ann. Rev. Fluid Mech.* 12, pp. 435 – 476, (1980).
16. Lovvorn J., Liggins G. A., Borstad M. H., Calisal S. M., Mikkelsen J., "Hydrodynamic drag of diving birds: effects of body size, body shape and feathers at steady speeds", *J. Exp. Biol.* 204, pp. 1547 – 1557, (2001).
17. Tran-Cong S., Gay M., Michaelides E. E., "Drag coefficients of irregularly shaped particles", *Powder Technol.* 139, pp. 21 - 32, (2004).
18. Qi J., Wang L., Yan F., Xue Q., "The tribological performance of DLC-based coating under the solid–liquid lubrication system with sand-dust particles", *Wear* 297, pp. 972 – 985, (2013).
19. Yan F., Li C., "A comparative investigation of the wear behavior of PTFE and PI under dry sliding and simulated sand-dust conditions", *Wear* 266, pp. 632 – 641, (2009).
20. Qi J., Wang L., Yan F., Xue Q., "Ultra-high tribological performance of magnetron sputtered a - C:H films in sand-dust environment", *Tribology Letters*, 38, pp. 195 – 203, (2010).
21. Qi J., Liu H., Luo Y., Zhang D., Wang Y., "Influences of added sand-dust particles on the tribological performance of graphite-like coating under solid–liquid lubrication", *Tribology International*, 71, pp. 69 – 81, (2014).